Agricultural and Forest Meteorology 265 (2019) 269–279

Contents lists available at ScienceDirect

Agricultural and Forest Meteorology

journal homepage: www.elsevier.com/locate/agrformet

Dynamic and thermodynamic changes conducive to the increased occurrence of extreme spring fire weather over western Canada under possible anthropogenic climate change

Xuezhi Tan[a,b,*], Shu Chen[c], Thian Yew Gan[b], Bingjun Liu[a], Xiaohong Chen[a]

[a] Department of Water Science and Engineering, School of Civil Engineering, Sun Yat-sen University, Guangzhou, 510275, PR China
[b] Department of Civil and Environmental Engineering, University of Alberta, Edmonton, Alberta T6G 2W2, Canada
[c] State Key Laboratory of Water Resources and Hydropower Engineering Science, Wuhan University, Wuhan, 430072, PR China

ARTICLE INFO

Keywords:
Dynamic changes
Thermodynamic changes
Anthropogenic climate change
Extreme fire
Western Canada

ABSTRACT

On May 2016 an extreme large wildfire affected Fort McMurray of Canada, leading to the largest wildfire evacuation and the costliest natural disaster in Canadian history. This wildfire was caused by extremely warm and dry weather conditions in spring. Here we investigate thermodynamic and dynamic (atmospheric circulation) conditions, and teleconnections conducive to extreme wildfire climate of western Canada since 1871. Results show that the extreme wildfire was very likely an outcome of anthropogenic effects that increase the occurrence of a persistent upper ridge associated with a warm and dry weather over western Canada. Changes in dynamic conditions decreased temperature and increased precipitation, while changes in thermodynamic conditions increased temperature and decreased precipitation. Thus the observed increase in temperature and decrease in precipitation on 26 April–15 May over western Canada were caused by changes in thermodynamic conditions. Although the Pacific North American (PNA) pattern was teleconnected with the occurrence of certain synoptic circulation patterns over western Canada, changes in the occurrence of the synoptic circulation pattern associated with the extreme wildfire cannot be explained by increased occurrences of the positive phase of PNA. The El Niño-Southern Oscillation and the Pacific Decadal Oscillation have not been found to have contributed to wildfire weather in western Canada. The spring warming and drying trends since 1871 over western Canada cannot be attributed to changes in common teleconnections.

1. Introduction

Although fire is a natural and necessary component of boreal forest ecosystems (e.g., fire shapes landscape diversity, affecting the carbon cycle, controls insects and diseases, and maintains biological diversity), fire also represents a threat to human life, property, and valuable commercial resources. The wildfire occurred in Fort McMurray which is located in the northeast of Alberta, Canada. The wildfire began on May 1, 2016 and swept through the nearby community in three days. It thus forced more than 88,000 people to flee their homes, resulting in the largest wildfire evacuation in Canada. The total insurable losses amount to $3 billion (U.S. dollars) which is the costliest insured claims disaster in Canadian history (Kochtubajda et al., 2017).

Working on the fuel (mostly vegetation), weather and climate conditions are the essential biophysical factors that control wildfire activity, even though climate relevance to wildfire occurrence varies across regions and landscapes (Moritz et al.,2012; Wang et al.,2017). Wildfire across boreal forests, tropical and subtropical moist broadleaf forests, and temperate broadleaf forests are highly sensitive to climate change (Bedia et al., 2015; Stocks et al.,1998). Since the 1970s, the highest increases in large wildfire activity occurred in mid-elevation, Northern Rockies forests, where increased spring and summer temperature and an earlier spring snowmelt are increasingly frequent (Gergel et al., 2017; Stocks et al., 1998; Westerling et al., 2006; Yoon et al., 2015). The proportion of days with the potential for unmanageable fire is projected to increase across Canada's forest (Wotton et al., 2017). The annual frequency of fire spread days in Canada could even increase 35–400 % by 2050 with the greatest increases over the Boreal Plains of Saskatchewan and Alberta (Wang et al., 2015). An increase in wildfire in Alaskan boreal forest and tundra ecosystems is also projected throughout the 21st century (Young et al., 2017). The increase in warm and dry weather has contributed to extreme wildfire events, but whether the weather conditions of extreme wildfire events are caused by natural variability or human-induced climate change

* Corresponding author.
E-mail address: tanxuezhi@mail.sysu.edu.cn (X. Tan).

https://doi.org/10.1016/j.agrformet.2018.11.026
Received 28 June 2018; Received in revised form 16 October 2018; Accepted 23 November 2018
Available online 28 November 2018
0168-1923/ © 2018 Elsevier B.V. All rights reserved.

remains unclear.

Therefore, we investigate the 2016 Fort McMurray wildfire from weather and climate perspectives, through analyzing synoptic circulation patterns that are associated with regional warm and dry weather conditions. From the weather perspective, we aim to advance the understanding of dynamic (atmospheric circulation) and thermodynamic (atmospheric moisture) conditions that contribute to warm and dry weather. Changes in precipitation and temperature are caused dynamically by changes in atmospheric circulation and thermodynamically by changes in conditions unrelated to atmospheric circulation such as changes in long-wave radiation from increasing greenhouse gases in atmosphere, or changes in moisture fluxes and/or latent heat resulting from changes in land cover (Horton et al., 2015; Seager et al., 2010). From the climate perspective, we analyze the long-term changes in dynamic and thermodynamic conditions to wildfire weather of western Canada over the period when the 2016 Fort McMurray wildfire occurred, and attribute changes in the occurrence of extreme wildfire weather to human impacts and natural climate variability.

Recent climate over western Canada has become systematically warmer and drier (Szeto et al., 2016) partly due to the tropical and North Pacific atmospheric dynamics that modulate their intra-seasonal and inter-annual variability (Newton et al., 2014). The relationships between continental-scale patterns of drought and large-scale climate variability such as El Niño-Southern Oscillation (ENSO), Pacific North American (PNA), Pacific Decadal Oscillation (PDO) North Atlantic Oscillation (NAO), and North Pacific Decadal Oscillation (NPD) can illustrate how large-scale inter-annual to multi-decadal climate variability drives fire at continental scales. Trends in large-scale climate variability due to global warming (e.g., a secular trend toward the positive PNA) will result in changes in widespread, synchronous fires in the future (Field et al., 2016; Kitzberger et al., 2007; Liu et al., 2017; Sauchyn et al., 2015). Majority of wildfire events are often associated with a small number of particular synoptic circulations that shows the synoptic climatology of wildfires (Lagerquist et al., 2017; Paschalidou and Kassomenos, 2016; Skinner et al., 1999). To improve wildfire management that highly relies on robust forecasts of changes in meteorological conditions, we identify the intra-seasonal and inter-annual variability related to the occurrence of synoptic circulations conducive to wildfire.

Although humans have affected fire regimes significantly by suppressing wildfires, providing ignition sources, and altering natural vegetation (Parisien et al., 2016), the influence of human-induced climate change on the area burned by forest fire in Canada over recent decades is also detectable with temperature change as an indicator (Gillett et al., 2004). The human-caused climate change contributed to nearly half of the forest fire area during 1984–2015 across western U.S. (Abatzoglou and Williams, 2016). However, the wildfire or drought weather conditions involve several climate variables (e.g., precipitation, humidity and wind) other than temperature, the human-induced signal of changes in drought condition may not be detectable because of large natural variability in these climate variables (Gergel et al., 2017; Stott et al., 2016; Szeto et al., 2016; Tan et al., 2018a). It is challenging to put an extreme event into the context of climate change for attributing that extreme climate event. The first approach is to identify anthropogenic signals by estimating fractions of attributable risk (Kirchmeier-Young et al., 2017; Stott et al., 2004; Tan et al., 2018a), while the second approach is to understand how physical processes at regional scales are impacted by climate change. Here we adopt the second approach. The weather conditions of Fort McMurray wildfire are put into the context of long-term variability and climate change across western Canada. Therefore, rather than detecting human-induced signals of changes in climate variables, we identify the human-induced signal of changes in synoptic circulation patterns that are identified using the self-organizing maps (SOMs) method.

Human-impacts on occurrences of extreme wildfire weather could be shown by the differences in the occurrence frequency of wildfire synoptic patterns in the period with and without significant human influences, e.g., pre-industry period and recent decades (Harrington et al., 2016). Changes in the occurrence of synoptic patterns are dynamic changes while changes in weather conditions (e.g., temperature and precipitation) showing in days when a particular synoptic pattern occurs are thermodynamic changes (Cassano et al., 2007; Horton et al., 2015). Changes in occurrences of extreme wildfire weather are attributed to dynamic changes and thermodynamic changes using the circulation-classification decomposition approach (Cassano et al., 2007).

The objective of this study is: (*i*) to find synoptic circulation patterns associated with occurrences of wildfire over western Canada; (*ii*) to relate the occurrence variability of these synoptic circulation patterns to large-scale climate teleconnections and anthropogenic climate change; and (*iii*) to partition the increased occurrence of extreme spring fire weather over western Canada to thermodynamic and dynamic contributions. Section 2 describes data and methodologies used in this analysis. Section 3 presents the results including synoptic circulation patterns and their associated spring fire weather conditions (e.g., precipitation and temperature). Section 4 discusses the results and the conclusions.

2. Data and methods

2.1. Synoptic circulation patterns

Circulations are derived from the daily 500 hPa geopotential heights of the NOAA-CIRES Twentieth Century (20C) Reanalysis (Compo et al., 2011) and considered over the period 1871–2012 on 26 April–15 May, and the area 30 °N–80 °N, 160 °W–80 °W. We focus on the weather and climate on 26 April–15 May when mid-spring extreme wildfire (e.g., the 2016 Fort McMurray) had developed. Because numerical weather prediction models produce representative pressure fields (Compo et al., 2011), applying a SOM to pressure fields could produce representative weather conditions conducive to the occurrence of wildfire (Kochtubajda et al., 2017). We use the SOM method (Cassano et al., 2007; Horton et al., 2015; Kohonen, 1998) to classify the daily pressure fields, i.e., 500 hPa geopotential heights, to obtain six primary synoptic circulation patterns. SOMs, a neural network algorithm, have been widely used to cluster high-dimensional meteorological data into several patterns (e.g., large-scale synoptic patterns). The SOM method has been shown to outperform principal component analysis, a traditional classification method, in identifying patterns of climatological data (Liu et al., 2006; Reusch et al., 2005). SOM is an unsupervised learning algorithm that does not require a priori knowledge of the types of circulation patterns and the specific geographic regions in which a circulation pattern might have occurred.

Long-term changes in the occurrence of synoptic circulation patterns in 1871–2012 are detected by the Mann-Kendall test. We use the 26 April–15 May 2016, 500 hPa geopotential height data of the NASA MERRA2 reanalysis (Gelaro et al., 2017) to show the atmospheric circulations in days of the wildfire (Fig. 1b). We compared the synoptic circulation patterns identified by the SOM method between the NOAA-CIRES 20C and the NASA MERRA2 reanalyses overlapped in 1980–2012, and results show that the daily circulation classification within these two reanalyses in 99.7% days are the same. Therefore, the circulation patterns of the 20C reanalysis (Fig. 2) could be used for analysis of the long-term changes in daily circulations.

Extreme climate events can then be attributed to certain synoptic patterns and changes in the occurrence of synoptic patterns under climate change could be estimated (Cassano et al., 2007). Specifically, extreme wildfire weather has been linked to particular regional synoptic patterns across the Eastern-Mediterranean region (Paschalidou and Kassomenos, 2016) and northern Alberta of Canada (Lagerquist et al., 2017) using the SOM method. We relate both temperature and precipitation over western Canada to synoptic patterns identified by SOMs. The occurrence of weather conditions conducive to extreme

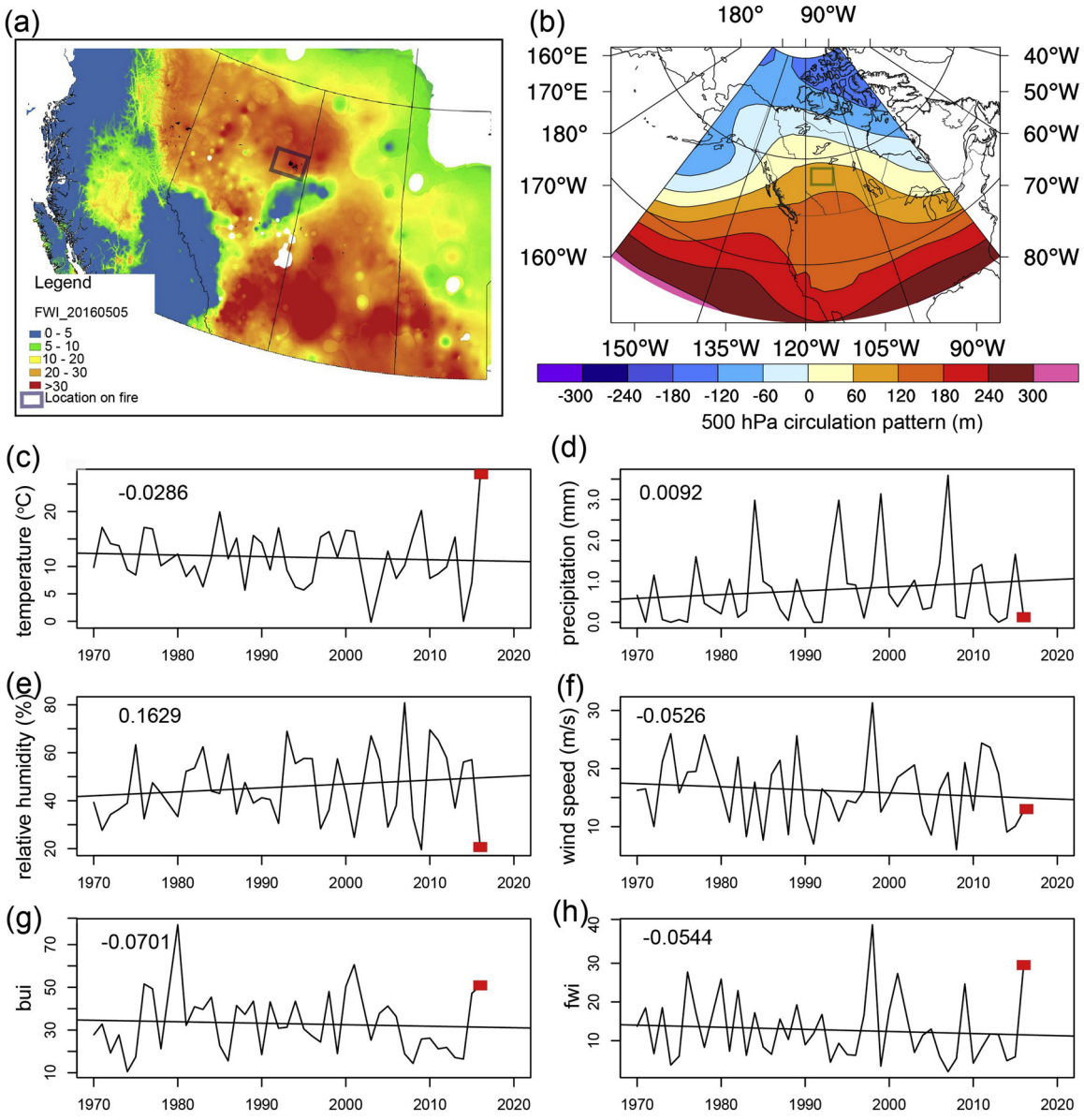

Fig. 1. Weather conditions for 2016 Fort McMurray Wildfire. (a) Map of Fire Weather Index on May 5th, 2016 (FWI_20160505) representing fire weather conditions over western Canada (adapted from Nature Resources Canada). The location of the Fort McMurray wildfire is shown in the green rectangle. The four weather stations used for estimate fire weather indices were shown in the green rectangle. (b) Map of the 500 hPa circulation patterns shown by geopotential height data (26 April–15 May 2016) of MERRA2 reanalysis (Gelaro et al. 2017). The rectangle over northeastern Alberta in (a) and (b) shows the wildfire area of Fort McMurray where observed spatial averages of wildfire weather parameters are calculated. (c–h) Primary wildfire weather parameters time series of area-average in the period of 1970–2016 during 26 April–15 May for temperature (c), precipitation (d), relative humidity (e), wind speed (f), the wildfire Buildup Index (bui; g), and the Canadian Forest Fire Weather Index (fwi; h). Linear trend (numbers over the topleft of each figure; year^{-1}) of the time series is also shown in the Fig. 1c–h. Values for the weather parameters in 2016 are denoted with red squares (For interpretation of the references to colour in this figure legend, the reader is referred to the web version of this article).

wildfire over western Canada is represented by the occurrence of the wildfire synoptic patterns that are similar to those occurred in days of the 2016 Fort McMurray wildfire and mostly favorable to the occurrence of extreme wildfire.

2.2. Surface climate

We used in situ weather measurements and wildfire weather index (Van Wagner, 1987) values (Fig. 1a and c–h) for four weather stations near Fort McMurray provided by the Canadian Wildland Fire Information System, Nature Resources Canada. We select four stations on the basis of (*i*) nearby region of wildfire occurred with longitudes between 115 °W and 110 °W and latitudes between 54 °N and 60 °N, (*ii*) the availability of more than 95% of daily values for temperature, precipitation, wind speed and relative humidity data during the wildfire season (April to October) between 1970 and 2016 for a reliable estimate of the long-term daily wildfire weather conditions, including both climatology and anomalies. We average the weather parameter and wildfire weather index values across four stations. Station data were only used to describe the hydrometeorological conditions for 2016 wildfire in Fort McMurray that were discussed in Section 3.1. However, to relate surface climate to synoptic circulation patterns, we use gridded temperature and precipitation data from the 20C reanalysis to maintain the physical consistency between surface climate and synoptic circulations.

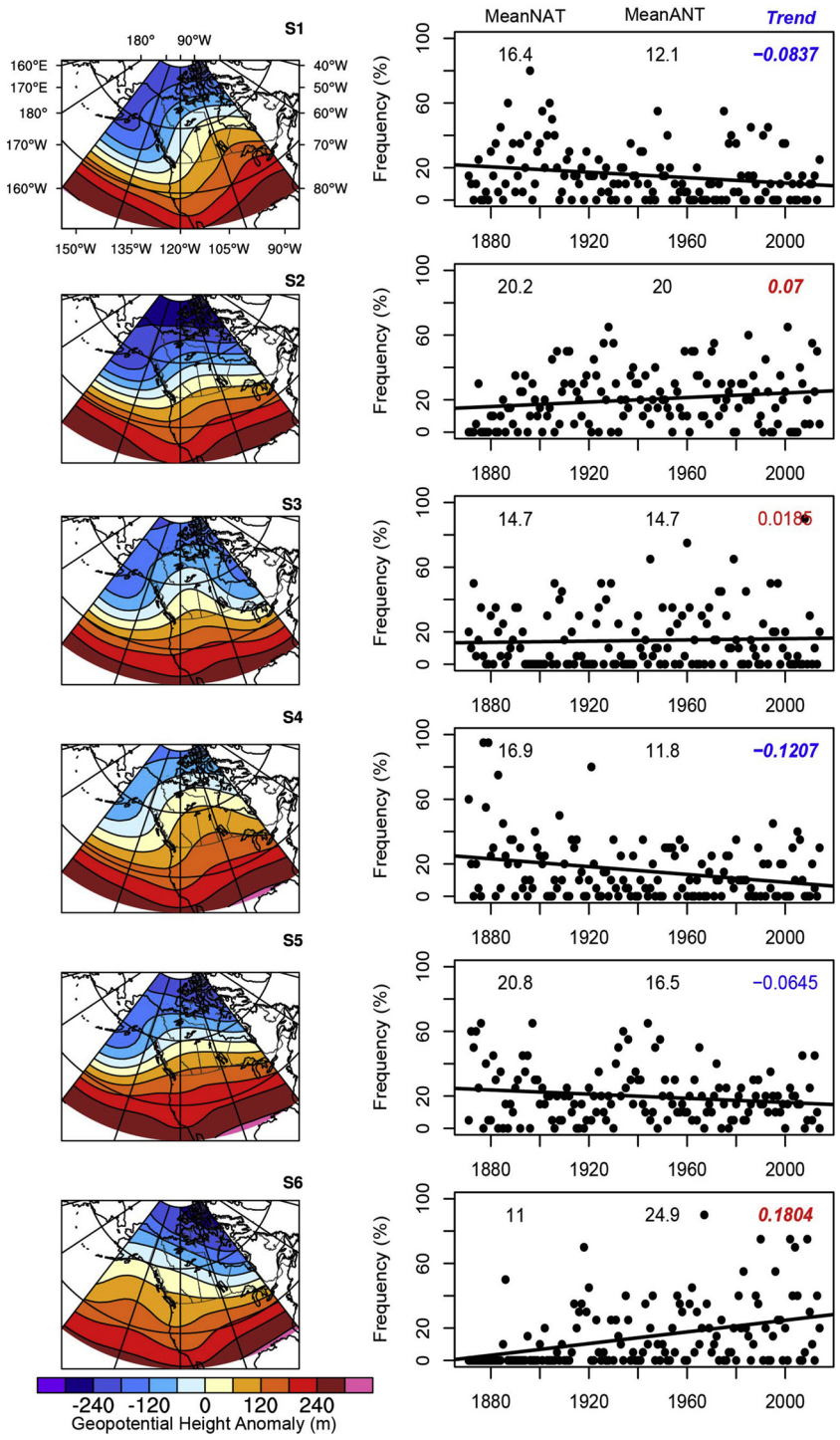

Fig. 2. Changes in occurrences of circulation patterns. (First column) Maps of 500 hPa circulation patterns obtained from the circulation clustering using the self-organizing map method with the geopotential height data of the Twentieth Century Reanalysis (Compo et al., 2011), in 1871–2014 on 26 April–15 May. (Second column) The time series of occurrence frequency of circulation patterns from 1871 to 2014. The mean occurrence frequency of patterns in 1871–1978 (MeanNAT) and 1979–2014 (MeanANT), and the trend of occurrence frequency are shown in the top of the figure. Statistically significant trends at the significance level of 0.05 are indicated with italic numbers. The positive (negative) trends or contributions are shown in red (blue) numbers (For interpretation of the references to colour in this figure legend, the reader is referred to the web version of this article).

2.3. Human-induces changes in occurrences of synoptic circulations

The 20C reanalysis has the longest climate data starting from 1871 within all reanalysis data (e.g., ERA-Interim, MERRA2 and CFSR, etc.). Using the longest circulation data make us identify possible effects of anthropogenic impacts on changes in circulation patterns by comparing the occurrence frequency of certain atmospheric circulation patterns between two time periods: 1871–1978 (“early-climate”) and 1979–2012 (“recent-climate”). The recent-climate is treated as a representative analog of the present-day climate, while the earlier period is intended to represent a climate with a much smaller influence from anthropogenic factors. Since each day’s circulation corresponds to one of these six circulation patterns, we estimate the occurrence frequency of each circulation pattern on each year and its changes from 1871 to 2012 and from early-climate to recent-climate (Fig. 2). We use the two-sample nonparametric Kolmogorov–Smirnov (KS) test to detect differences in the occurrence frequency of circulation patterns between the early-climate and recent-climate. By comparing the early-climate and recent-climate, we attribute regional climate change to anthropogenic factors using the circulation-classification method of SOM as in the analysis of the North Island Drought of 2013 (Harrington et al., 2016).

2.4. Teleconnections of synoptic circulation occurrences

We use climate indices that represent the above five large-scale climate anomalies or teleconnections (i.e., ENSO, PNA, PDO, NAO and NPD) to evaluate their influence on occurrences of synoptic circulation patterns and weather conditions related to them for western Canada. The Southern Oscillation Index (SOI) (Ropelewski and Jones, 1987) is used to represent ENSO. The cold (warm) ENSO phase, i.e., La Niña (El Niño), is represented by positive (negative) values of the SOI. Monthly values of the SOI, PDO and NAO indices in 1871–2012, PNA index values in 1948–2012 and NPD index values in 1899–2012 are obtained from the Climate Explorer. These indices values are the longest data we can collect. Instead of using consistent data within the same period for the analyzed climate indices, we use data of different period to analyze the long-term variability and teleconnections of wildfire weather. We divide each monthly teleconnection into three phases based on thresholds of 16th and 84th percentiles, i.e., positive, neutral, and negative, respectively, for the above periods considered for climate indices. This procedure was widely used to categorize teleconnections (Bonsal et al., 2017; Newton et al., 2014). We link January-February average SOI, PDO, NAO, NPD and PNA conditions to each synoptic circulation pattern as composite teleconnection conditions, as those teleconnections are usually strongest in January-February (Bonsal et al., 2001; Tan et al., 2016, 2018b). We use the two-sample non-parametric KS test to evaluate differences in synoptic type frequency distributions for each positive–negative pair at the 0.05 significance.

2.5. Partition of surface climate changes

The contribution of large-scale dynamic and thermodynamic conditions to temperature and precipitation anomalies of 1871–2012 is estimated using the decomposition approach (Cassano et al., 2007; Horton et al., 2015). To relate atmospheric circulation patterns to weather regimes, we derive composite anomalies of temperature and precipitation (expressed as percentage departures from normal) for each circulation pattern, using temperature and precipitation data of 20C reanalysis to keep the physical consistence between climate variables. We also estimate changes in temperature and precipitation of western Canada in days when a particular circulation occurred over the 1871–2012 period. To partition changes in temperature and precipitation into three components: (*i*) dynamic changes associated with individual SOM circulation patterns, (*ii*) thermodynamic changes associated with temperature or precipitation occurred in individual circulation patterns, and (*iii*) a combination of both dynamic and thermodynamic changes. Following Cassano et al. (2007):

$$T = \sum_{i=1}^{K} T_i f_i \tag{1}$$

$$P = \sum_{i=1}^{K} P_i f_i \tag{2}$$

where T and P are temperature and precipitation, respectively; f_i is the occurrence frequency of the SOM pattern i; T_i and P_i is the regional area-weighted average temperature and precipitation when SOM pattern i occurs; and K is the total number of SOM patterns. We can decompose T, P and f into time mean and deviation components:

$$T = \sum_{i=1}^{K} (\overline{T_i} + T_i')(\overline{f_i} + f_i') \tag{3}$$

$$P = \sum_{i=1}^{K} (\overline{P_i} + P_i')(\overline{f_i} + f_i') \tag{4}$$

Now we can differentiate above equations with respect to time, with mean values as constants:

$$\frac{dT}{dt} = \sum_{i=1}^{K} \left(\overline{f_i} \frac{dT_i'}{dt} + \overline{T_i} \frac{df_i'}{dt} + \frac{d(T_i' f_i')}{dt} \right) \tag{5}$$

$$\frac{dP}{dt} = \sum_{i=1}^{K} \left(\overline{f_i} \frac{dP_i'}{dt} + \overline{P_i} \frac{df_i'}{dt} + \frac{d(P_i' f_i')}{dt} \right) \tag{6}$$

The derivative on the left-hand side of Eqs. (5) and (6) is the area-weighted average changes in temperature and precipitation for all days, respectively. From left to right, the summation on the right-hand side is the thermodynamic, dynamic and interaction contributions for days when a SOM pattern, *i*, occurs. The thermodynamic contribution of a circulation pattern to changes in precipitation and temperature assumes that each SOM pattern is invariant in time in terms of its occurrence, and those changes in temperature and precipitation, respectively, that result from this pattern are the result of changes in thermodynamic conditions, such as moisture fluxes and/or latent heat resulting from changes in land cover and increasing greenhouse gases in atmosphere. The product of changes in the daily temperature and precipitation occurred in a SOM pattern, *i*, and the mean occurrence of that pattern shows the thermodynamic contribution associated with that circulation pattern. Changes in daily temperature and precipitation within each pattern were computed by calculating the least-squares linear trend in area-weighted daily temperature (precipitation) as shown in Figs. 5 and 6, respectively.

The dynamic contribution of a circulation pattern to changes in temperature (precipitation) assumes that changes in the occurrence frequency of a circulation pattern modify the daily temperature (precipitation) that is associated with that pattern. The product of changes in the occurrence frequency of a circulation pattern and the mean daily temperature (precipitation) per pattern occurrence shows the dynamic contribution associated with that circulation pattern. The third term represents the combined contribution to changes in temperature (precipitation) which arises from changes in pattern frequency acting on changes in daily temperature (precipitation). The combined contribution only amounts to less than 10% of the total changes and is much lower than the thermodynamic and dynamic changes (Cassano et al., 2007; Horton et al., 2015).

3. Results

3.1. Hydrometeorological conditions for 2016 wildfire in Fort McMurray

The weather condition was extremely warm and dry during 26 April–15 May 2016 and contributed to the occurrence of a severe wildfire of Fort McMurray (Fig. 1a): (*i*) the highest surface daily maximum air temperature of almost 30 °C since 1970, which was ~300% of the 1970–2000 average (Fig. 1c); (*ii*) the long consecutive dry days (> 15 days); (*iii*) the second lowest dry air mass since 1970 with a relative humidity below 20% (Fig. 1e); and (*iiii*) wind sweeping over the Fort McMurray region, although the regional and temporal average of wind speed was slightly lower than normal values (Fig. 1f).

On May 3, the surface air temperature climbed to 32.8 °C, accompanied by an extremely low relative humidity (12%). The situation intensified on May 4 when temperature reached 31.9 °C and winds gusted to 72 km h^{-1}, which contributed to the fire's rapid growth as both the Buildup Index (bui; > 50) and the Fire Weather Index (fwi; > 30) were extremely high (Fig. 1a and g–h) which corresponds to the > 90 and 95th percentile of the observed values. The bui shows the total amount of fuel available for combustion. The fwi shows the fire intensity that combines the expected rate of fire spread and the total amount of fuel available for combustion. The winter preceding the fire was warmer and drier than normal, so the paltry winter snowpack melted quickly and plenty of uncovered fuel was left for wildfires (Kochtubajda et al., 2017). Seasonally, winter 2015/16 was the 18th driest since 1948, with the national average precipitation 95% of the 1961–90 average (Blunden and Arndt, 2017). Combined with dry weather, this created a "perfect storm" of conditions for an explosive wildfire to occur over northern Alberta. However, from 1970 to 2016, the observed data during 26 April–15 May showed a decrease in

temperature, wind speed and wildfire weather indices (i.e., bui and fwi), but an increase in precipitation and relative humidity. This means that the weather conditions should be less prone to wildfire on 26 April - 15 May. However, the extremely large value of fwi associated with extreme wildfire in summer and fall mostly occurred in recent two decades.

The atmospheric circulation pattern displayed a ridge with large-amplitude and its axis pointing north over the wildfire region of Fort McMurray (Fig. 1b). This circulation pattern is associated with a drier and warmer climate that is characterized by positive temperature and negative precipitation anomalies over northern Alberta based on the analysis of the climate data of 1950–2010 (Bonsal et al., 2017). Since geopotential heights increased significantly over northern Pacific while decreased over central and eastern North America on 26 April–15 May (Fig. 2a), there were changes in atmospheric circulations and associated wildfire weather regimes. On 26 April–15 May over western Canada, the temperature has increased (Fig. 2b) and the precipitation has decreased (Fig. 2c) since 1871.

3.2. Synoptic circulation patterns and teleconnections to wildfire weather

We cluster the daily 500 hPa geopotential heights (Compo et al., 2011)over the period 1871–2012 on 26 April–15 May and the area 30 °N–80 °N, 160 °W–80 °W, to six circulation patterns that capture different synoptic-scale circulation patterns over western Canada including troughing, ridging, and zonal flows (Fig. 3). The occurrence of four out of six circulation patterns changed statistically significantly. Differences in the occurrence of five circulation patterns between early-climate (1871–1978) to recent-climate (1979–2012) periods are also statistically significant as detected. This shows anthropogenic impacts on atmospheric circulation changes. In particular, Patterns S4 and S5 occurring ~30% of the time displays a large-amplitude ridge with its axis over Alberta. The atmospheric circulations on 26 April - 15 May 2016 were most similar to Pattern S4 (Figs. 1b and 2).

From the perspective of the particular Fort McMurray wildfire only, a near-record strong El Niño event, a strong positive phase of the PDO in 2015, and a second and third highest January and February PNA values since 1950, respectively, were followed by the abnormally dry and warm conditions over the Fort McMurray area or western Canada (Kochtubajda et al., 2017). However, shown by long-term statistical analysis, the effects of five large-climate anomalies, ENSO, PDO, NAO, NPD and PNA on the occurrence of all six synoptic circulation patterns were generally not statistically significant (Figs. 4a–e). Therefore, we cannot attribute to the 2016 Fort McMurray wildfire to the extreme El Niño in previous winter. However, the PNA showed a strong teleconnection with the occurrence of five out of six synoptic circulation patterns (Fig. 4e). Patterns S2 and S5 (S3 and S6) tended to occur in the negative (positive) phase of PNA. The PNA index values have statistically significantly increased from 1940 to the present (Fig. 4f). Therefore, the occurrence of Patterns S3 and S6 have increased and the occurrence of Pattern S5 has decreased (Fig. 2). This shows certain predictability of the occurrence of synoptic circulation patterns on 26 April–15 May 2016 over western Canada based on the PNA teleconnection. Although the effect of PNA on the occurrence of Pattern S4 was not statistically significant, Pattern S4 which was associated with the 2016 Fort McMurray wildfire was more likely to occur in the positive phase of PNA. However, as the decreased occurrence of Pattern S4 did not coincide with the increased values of PNA, changes in occurrence Pattern S4 cannot be explained by the variability of PNA.

3.3. Thermodynamic and dynamic contribution to increased wildfire weather

The occurrence frequency of Pattern S4 statistically significantly decreased from 1871 to 2012 by 0.12% per year and decreased from early-climate to recent-climate by 5.1%. The corresponding

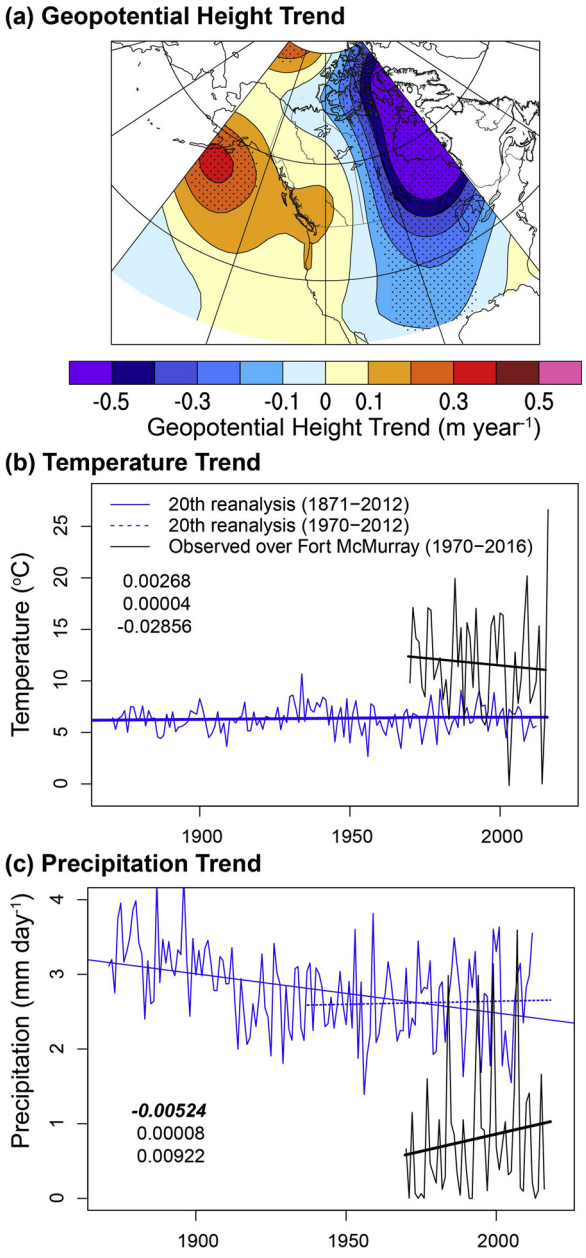

Fig. 3. Changes in weather conditions in spring over Fort McMurray (green rectangle) and western Canada (red frame). (a) Maps of the trend of 500 hPa geopotential height over the west of North America. (b and c) The area-weighted average of temperature (b) and precipitation (c) over western Canada. The three numbers shown in Figs. 3b-c from the top to the bottom denotes the slope of least-squares straight lines for the 20th reanalysis (1871–2012), the 20th reanalysis (1871–2012), and the observed over the Fort McMurray (1970–2016), respectively. Statistically significant trends are shown in bold italic numbers. Note that station data (green rectangle) are only for the area of the Fort McMurray while the reanalysis data (red frame) are for the whole western Canada. Therefore, temperature and precipitation data shown in blue and black lines are not directly comparable (For interpretation of the references to colour in this figure legend, the reader is referred to the web version of this article).

temperature anomalies of Pattern S4 were characterized by warmer conditions over western Canada including the Fort McMurray wildfire region (Fig. 5), since the ridge could descend air currents and lead to higher surface temperature. However, the temperature in days occurring with Pattern S4 statistically significantly decreased by 0.005 °C year^{-1} (Fig. 5). Therefore, both thermodynamic (negative temperature

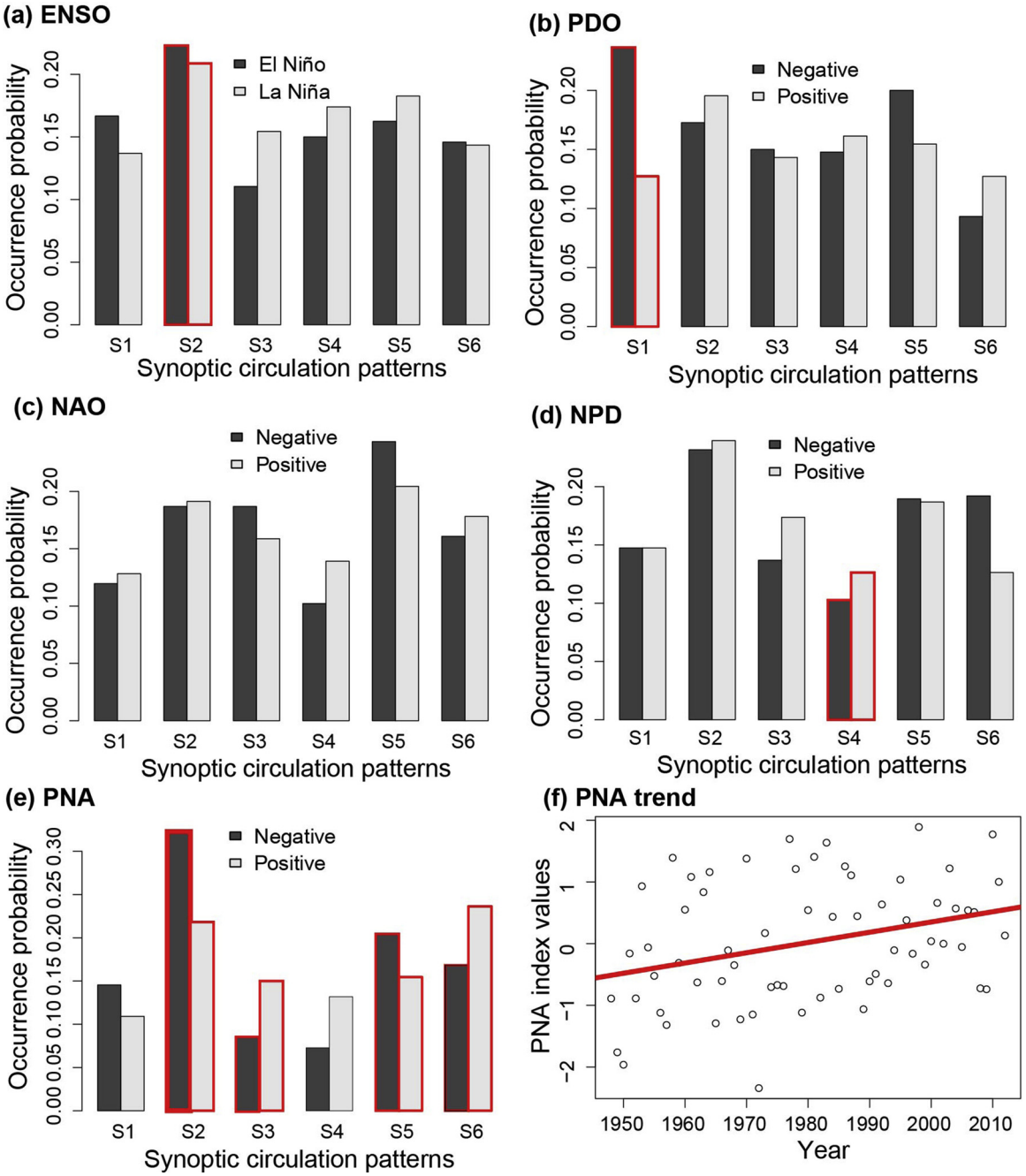

Fig. 4. Teleconnections to occurrences of circulation patterns.Comparison of synoptic type frequency distribution between positive and negative teleconnection conditions of ENSO (a), PDO (b), NAO (c), PDO (d) and PNA (e). Statistically significant differences in synoptic type frequency distributions detected by the two-sample Kolmogorov–Smirnov test are shown with red frames over the pair-wise bars. (f) Trends of PNA values (For interpretation of the references to colour in this figure legend, the reader is referred to the web version of this article).

trend times positive pattern occurrence) and dynamic changes (negative pattern occurrence trend times positive temperature anomaly) in Pattern S4 contributed to the decrease in temperature. However, the temperature increased under all other five circulation patterns (the second column of Fig. 5). The thermodynamic (dynamic) changes contribute to an increase (decrease) in temperature by 15.5 (12.6) ˚C from 1871 to 2012, with an overall increase of 2.9 ˚C on 26 April–15 May over western Canada. This indicates that thermodynamic changes had substantially enhanced the warmer weather for wildfire as temperature increase.

However, precipitation over northern Alberta in days occurring with Pattern S4 had decreased, even though the decreasing trend was not statistically significant (Fig. 6). Moreover, Pattern S4 corresponds to positive precipitation anomalies over northern Alberta (Fig. 6). Both thermodynamic and dynamic changes contributed to a decrease in precipitation over northern Alberta. However, thermodynamic changes contributed to an increase in precipitation in Pacific coastal regions of Canada (western British Columbia). This increase was considerably larger than the decrease in Alberta and therefore resulted in an overall increase in areal mean precipitation over western Canada because of thermodynamic changes (Fig. 6). The decrease in precipitation associated with Pattern S4 indicates the more likely occurrence of wildfire weather. In other five circulation patterns, Patterns S1 and S3 were also associated with a decrease in precipitation over northern Alberta, while

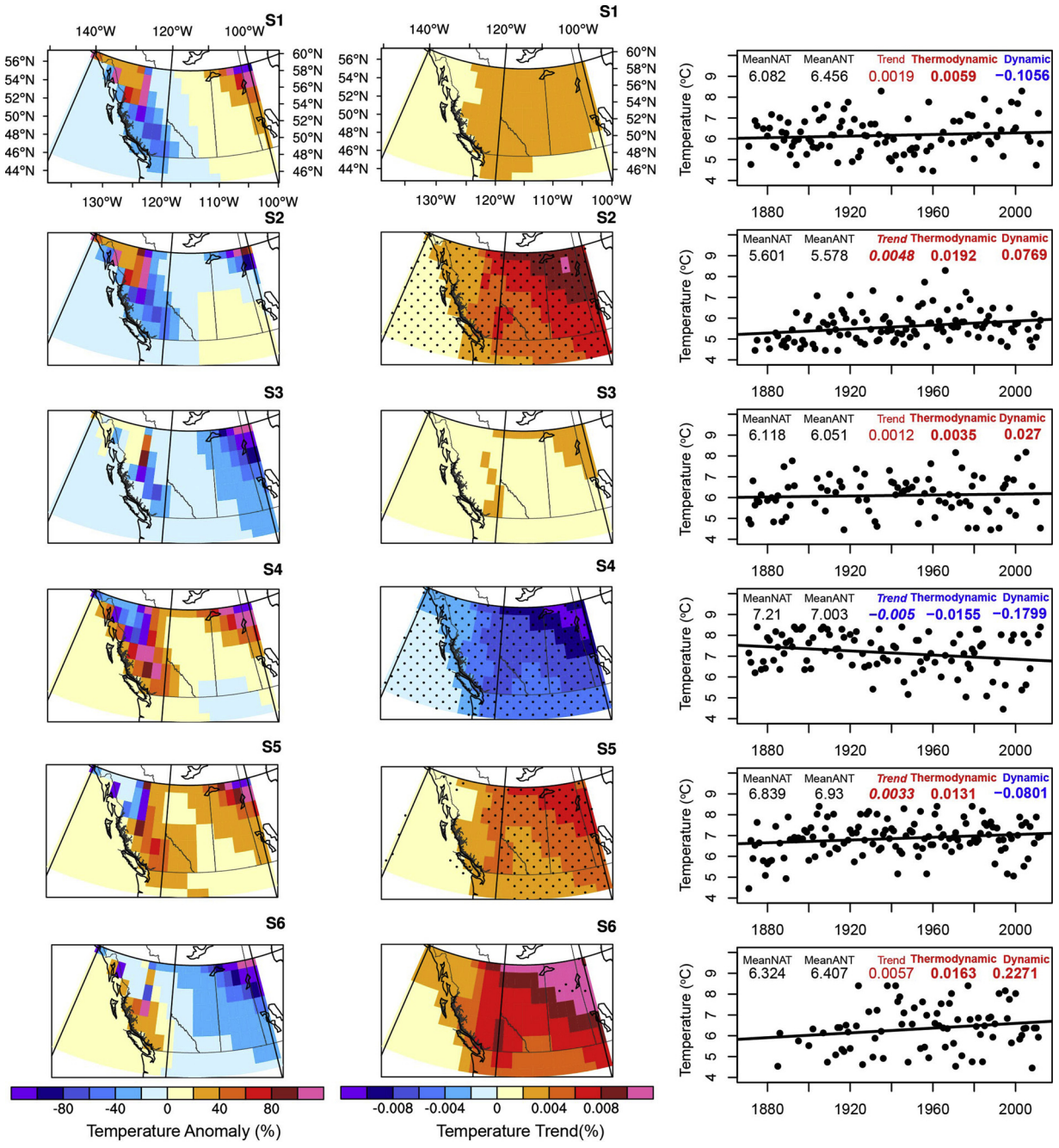

Fig. 5. Changes in temperature associated with circulation patterns. (First column) Maps of the temperature anomalies for days when a circulation pattern occurred relative to the mean value of the temperature for all days in 1871–2014 on 26 April–15 May. (Second column) Maps of the trends of temperature in days when a circulation pattern occurred from 1871 to 2014. Regions with statistically significant trends in temperature under a circulation pattern are stippled. (Third column) The time series of the area-weighted average of temperature over western Canada in days when a circulation pattern occurred from 1871 to 2014. The area-weighted averages of temperature of the entire western Canada in days when a circulation pattern occurred in 1871-1978 (MeanNAT) and 1979–2014 (MeanANT), and their trends are shown in the top of the figures. The contribution of changes in thermodynamic and dynamic conditions to changes in area-weighted average of temperature is also shown in figures. The unit for trend and contribution is °C year^{-1}. Statistically significant trends at the significance level of 0.05 are indicated with italic numbers. The positive (negative) trends or contributions are shown in red (blue) numbers (For interpretation of the references to colour in this figure legend, the reader is referred to the web version of this article).

Patterns S2, S5 and S6 corresponded to an increase in precipitation over northern Alberta. For entire western Canada, thermodynamic (dynamic) changes contributed to a decrease (increase) in precipitation by 6.62 (5.32) mm from 1871 to 2012, with an overall decrease of 1.30 mm on 26 April–15 May over western Canada. This indicates that thermodynamic changes had substantially enhanced the drier weather for wildfire as precipitation decrease across western Canada. Thus, thermodynamic changes contributing to the increased temperature and decreased precipitation were related to the increased occurrence frequency of extreme wildfire weather (e.g., Fort McMurray wildfire) over western Canada.

4. Discussion and conclusions

Since wildfire weather shows multifaceted characteristics and forcings, it is a challenging task to exactly attribute an extreme wildfire

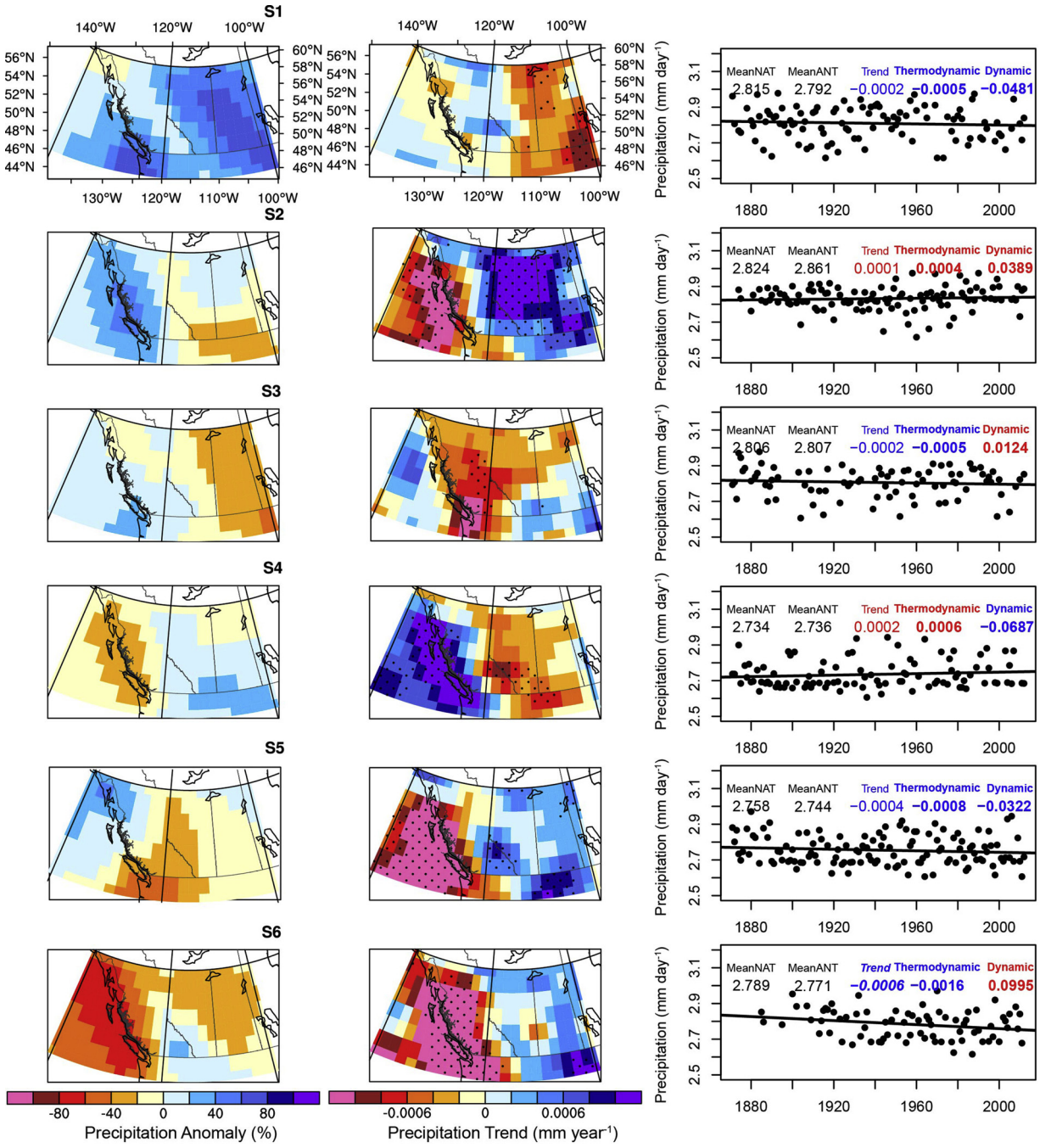

Fig. 6. Changes in precipitation associated with circulation patterns. (First column) Maps of the precipitation anomalies for days when a circulation pattern occurred relative to the mean value of the precipitation for all days in the period of 1871–2014 during 26 April–15 May. (Second column) Maps of the trends of precipitation in days when a circulation pattern occurred from 1871 to 2014. Regions with statistically significant trends in precipitation under a circulation pattern are stippled. (Third column) The time series of the area-weighted average of precipitation over western Canada in days when a circulation pattern occurred from 1871 to 2014. The area-weighted averages of precipitation of the entire western Canada in days when a circulation pattern occurred in 1871–1978 (MeanNAT) and 1979–2014 (MeanANT), and their trends are shown in the top of the figures. The contribution of changes in thermodynamic and dynamic conditions to changes in area-weighted average of precipitation is also shown in figures. The unit for trend and contribution is mm day^{-1} year^{-1}. Statistically significant trends at the significance level of 0.05 are indicated with italic numbers. The positive (negative) trends or contributions are shown in red (blue) numbers (For interpretation of the references to colour in this figure legend, the reader is referred to the web version of this article).

event to changes in weather regimes. The 2016 Fort McMurray wildfire was caused by a combination of extremely low snowpack in the winter preceding the fires and consecutive warm and dry weather in late April and early May. It is expected that as the planet continues to warm and spring snowpack disappears and warm temperature persists, this type of spring fires will likely become more common and intense (Gergel et al., 2017; Westerling et al., 2006). Even though the spring wildfire risk across small regions surrounding Fort McMurray has decreased over 1970–2016, extremely large spring wildfire risk occurred most in recent two decades. Warmer and drier spring over western Canada since 1871 has become more favorable to occurrences of extreme wildfire events.

Our analysis suggests that the occurrence of most circulation patterns changed statistically significantly from early-climate to recent-climate, which shows that the extreme wildfire weather (e.g., Fort

McMurray wildfire 2016) was likely an outcome of anthropogenic effects that increase the occurrence of a persistent upper ridge and a warm and dry climate. For the whole of western Canada, the dynamic contribution to the decreased temperature and increased precipitation were not sufficient to offset the thermodynamic contribution to the increased temperature and decreased precipitation. Thus, the observed increased temperature and decreased precipitation on 26 April–15 May were caused by changes in thermodynamic conditions. We conjecture that this could be due to decreased precipitation rates within the circulation patterns which are limited by moisture supply and convey less moisture, albeit temperature had increased.

The observed trend in temperature and precipitation over regions near Fort McMurray is opposite to those over entire western Canada, and the weather conditions show different trends in different time periods (e.g., early-climate to recent-climate). The analysis on western Canada averages out substantial temporal variability that exists in local temperature and precipitation (Fig. 3-c). The attribution of wildfire weather changes could be dependent on the region and period analyzed, although this requires more studies on fine-scale spatiotemporal temperature and precipitation processes. However, our analysis shows how the atmospheric circulation patterns and thermodynamic conditions result in a warm and dry climate conducive to the occurrence of wildfire, and their changes as well.

The large-scale climate variability is known to modulate the hydroclimate of western Canada (Gan et al., 2007; Newton et al., 2014; Tan et al., 2016). For example, the natural El Niño and the negative PDO phase resulted in a dry fall and winter season and followed by a warm spring over western Canada (Bonsal et al., 2001; Tan et al.,2016). However, for the period when the Fort McMurray wildfire 2016 occurred, we have not found significant differences in the occurrence of circulation patterns between different phases of ENSO and PDO, and so ENSO and PDO have not been found to have contributed to the wildfire weather of western Canada. Although PNA was teleconnected with the occurrence of certain synoptic circulation patterns over western Canada, changes in the occurrence of the synoptic circulation pattern that is associated with the 2016 Fort McMurray wildfire cannot be explained by the increased occurrence of the positive phase of PNA. Hence, we cannot attribute the warming and drying trends in spring over western Canada since 1871 to changes in common large-scale climate variabilities.

Acknowledgments

We thank Mr. Bo Lu from the Northern Forestry Center (http://cwfis.cfs.nrcan.gc.ca/home) for providing wildfire weather data and Mr. Anthony Liu from the Environment and Climate Change Canada (ECCC) for providing the observed climate data. The first author was partly funded by the China Scholarship Council (CSC) of P.R. China and the University of Alberta. This research is supported by Natural Science and Engineering Research Council of Canada, the National Natural Science Foundation of China (Grant Nos. 91547108, 51822908 and 51809295) and the National Key Research and Development Program of China (2017YFC0405900 and 2016YFC0401300). Climate indices data were downloaded from https://climexp.knmi.nl/selectindex.cgi?id=someone@somewhere. The MERRA2 reanalysis data were downloaded from https://gmao.gsfc.nasa.gov/reanalysis/MERRA-2/and the 20C reanalysis data were downloaded from https://www.esrl.noaa.gov/psd/data/20thC_Rean/.

References

Abatzoglou, J.T., Williams, A.P., 2016. Impact of anthropogenic climate change on wildfire across western US forests. Proc. Natl. Acad. Sci. U. S. A. 113, 11770–11775.
Bedia, J., Herrera, S., Gutiérrez, J.M., Benali, A., Brands, S., Mota, B., Moreno, J.M., 2015. Global patterns in the sensitivity of burned area to fire-weather: implications for climate change. Agric. Forest Meteorol. 214 (215), 369–379.
Blunden, J., Arndt, D.S., 2017. State of the Climate in 2016. Bull. Am. Meteorol. Soc. 98, S1–S280.
Bonsal, B.R., Shabbar, A., Higuchi, K., 2001. Impacts of low frequency variability modes on Canadian winter temperature. Int. J. Climatol. 21, 95–108.
Bonsal, B.R., Cuell, C., Wheaton, E., Sauchyn, D.J., Barrow, E., 2017. An assessment of historical and projected future hydro-climatic variability and extremes over southern watersheds in the Canadian Prairies. Int. J. Climatol. 37, 3934–3948.
Cassano, J.J., Uotila, P., Lynch, A.H., Cassano, E.N., 2007. Predicted changes in synoptic forcing of net precipitation in large Arctic river basins during the 21st century. J. Geophys. Res. 112, G04S49. https://doi.org/10.1029/2006jg000332.
Compo, G.P., et al., 2011. The Twentieth Century reanalysis project. Q. J. R. Meteorol. Soc. 137, 1–28.
Field, R.D., et al., 2016. Indonesian fire activity and smoke pollution in 2015 show persistent nonlinear sensitivity to El Nino-induced drought. Proc. Natl. Acad. Sci. U. S. A. 113, 9204–9209.
Gan, T.Y., Gobena, A.K., Wang, Q., 2007. Precipitation of western Canada: wavelet, scaling, multifractal analysis, and teleconnection to climate anomalies. J. Geophys. Res. 112, D10110. https://doi.org/10.1029/2006jd007157.
Gelaro, R., et al., 2017. The modern-era retrospective analysis for research and applications, Version 2 (MERRA-2). J. Clim. 30, 5419–5454.
Gergel, D.R., Nijssen, B., Abatzoglou, J.T., Lettenmaier, D.P., Stumbaugh, M.R., 2017. Effects of climate change on snowpack and fire potential in the western USA. Clim. Change 141, 287–299.
Gillett, N.P., Weaver, A.J., Zwiers, F.W., Flannigan, M.D., 2004. Detecting the effect of climate change on Canadian forest fires. Geophys. Res. Lett. 31, L18211. https://doi.org/10.1029/2004GL020876.
Harrington, L.J., Gibson, P.B., Dean, S.M., Mitchell, D., Rosier, S.M., Frame, D.J., 2016. Investigating event-specific drought attribution using self-organizing maps. J. Geophys. Res. Atmos. 121 (12) 766-712,780.
Horton, D.E., Johnson, N.C., Singh, D., Swain, D.L., Rajaratnam, B., Diffenbaugh, N.S., 2015. Contribution of changes in atmospheric circulation patterns to extreme temperature trends. Nature 522, 465–469.
Kirchmeier-Young, M.C., Zwiers, F.W., Gillett, N.P., Cannon, A.J., 2017. Attributing extreme fire risk in Western Canada to human emissions. Clim. Change 144, 365–379.
Kitzberger, T., Brown, P.M., Heyerdahl, E.K., Swetnam, T.W., Veblen, T.T., 2007. Contingent Pacific-Atlantic Ocean influence on multicentury wildfire synchrony over western North America. Proc. Natl. Acad. Sci. U. S. A. 104, 543–548.
Kochtubajda, B., Brimelow, J., Flannigan, M., Morrow, B., Greenhough, M.D., 2017. The extreme 2016 wildfire in Fort Mcmurray, Alberta, Canada. In "State of the climate in 2016. Bull. Am. Meteorol. Soc. 98, S176–S177.
Kohonen, T., 1998. The self-organizing map. Neurocomputing 21, 1–6.
Lagerquist, R., Flannigan, M.D., Wang, X., Marshall, G.A., 2017. Automated prediction of extreme fire weather from synoptic patterns in northern Alberta, Canada. Can. J. For. Res. 47, 1175–1183.
Liu, Z., et al., 2017. Pacific North American circulation pattern links external forcing and North American hydroclimatic change over the past millennium. Proc. Natl. Acad. Sci. U. S. A. 114 (13), 3340–3345.
Moritz, M.A., Parisien, M.-A., Batllori, E., Krawchuk, M.A., Van Dorn, J., Ganz, D.J., Hayhoe, K., 2012. Climate change and disruptions to global fire activity. Ecosphere 3https://doi.org/10.1890/es11-00345.1. art49.
Newton, B.W., Prowse, T.D., Bonsal, B.R., 2014. Evaluating the distribution of water resources in western Canada using synoptic climatology and selected teleconnections. Part 2: summer season. Hydrol. Process. 28, 4235–4249.
Parisien, M.-A., Miller, C., Parks, S.A., DeLancey, E.R., Robinne, F.-N., Flannigan, M.D., 2016. The spatially varying influence of humans on fire probability in North America. Environ. Res. Lett. 11, 075005. https://doi.org/10.1088/1748-9326/11/7/075005.
Paschalidou, A.K., Kassomenos, P.A., 2016. What are the most fire-dangerous atmospheric circulations in the Eastern-Mediterranean? Analysis of the synoptic wildfire climatology. Sci. Total Environ. 539, 536–545.
Reusch, D.B., Alley, R.B., Hewitson, B.C., 2005. Relative performance of self-organizing maps and principal component analysis in pattern extraction from synthetic climatological data. Polar Geogr. 29 (3), 227–251.
Ropelewski, C.F., Jones, P.D., 1987. An extension of the Tahiti-Darwin southern oscillation index. Mon. Weather Rev. 115, 2161–2165.
Sauchyn, D.J., St-Jacques, J.M., Luckman, B.H., 2015. Long-term reliability of the Athabasca River (Alberta, Canada) as the water source for oil sands mining. Proc. Natl. Acad. Sci. U. S. A. 112 (41) 12621-6.
Skinner, W.R., Stocks, B.J., Martell, D.L., Bonsal, B., Shabbar, A., 1999. The association between circulation anomalies in the mid-troposphere and area burned by wildland fire in Canada. Theor. Appl. Climatol. 63, 89–105.
Seager, R., Naik, N., Vecchi, G.A., 2010. Thermodynamic and dynamic mechanisms for large-scale changes in the hydrological cycle in response to global warming. J. Clim. 23, 4651–4668.
Stocks, B.J., et al., 1998. Climate change and forest fire potential in Russian and Canadian boreal forests. Clim. Change 8, 1–13.
Stott, P.A., Stone, D.A., Allen, M.R., 2004. Human contribution to the European heatwave of 2003. Nature 432, 610–614.
Stott, P.A., et al., 2016. Attribution of extreme weather and climate-related events. Wiley interdisciplinary reviews. Clim. Change 7, 23–41.
Szeto, K., Zhang, X., White, R.E., Brimelow, J., 2016. The 2015 extreme drought in western Canada. Bull. Am. Meteor. Soc. 97, S42–S46.
Tan, X., Gan, T.Y., Shao, D., 2016. Wavelet analysis of precipitation extremes over Canadian ecoregions and teleconnections to large-scale climate anomalies. J. Geophys. Res. Atmos. 121, 14469–14486.
Tan, X., Chen, S., Gan, T.Y., 2018a. Multi-model extreme event attribution of the weather conducive to the 2016 Fort McMurray wildfire. Agric. For. Meteorol. 260 (261), 109–117.

Tan, X., Gan, T.Y., Chen, Y.D., 2018b. Synoptic moisture pathways associated with mean and extreme precipitation over Canada for summer and fall. Clim. Dyn. https://doi.org/10.1007/s00382-018-4300-6.

Van Wagner, C.E., 1987. Development and Structure of the Canadian Forest Fire Weather Index System. Forestry Technical Report. pp. 35.

Wang, X., Thompson, D.K., Marshall, G.A., Tymstra, C., Carr, R., Flannigan, M.D., 2015. Increasing frequency of extreme fire weather in Canada with climate change. Clim. Change 130, 573–586.

Wang, X., et al., 2017. Projected changes in daily fire spread across Canada over the next century. Environ. Res. Lett. 12, 025005. https://doi.org/10.1088/1748-9326/aa5835.

Westerling, A.L., Hidalgo, H.G., Cayan, D.R., Swetnam, T.W., 2006. Warming and earlier spring increase western US forest wildfire activity. Science 313, 940–943.

Wotton, B.M., Flannigan, M.D., Marshall, G.A., 2017. Potential climate change impacts on fire intensity and key wildfire suppression thresholds in Canada. Environ. Res. Lett. 12, 095003. https://doi.org/10.1088/1748-9326/aa7e6e.

Yoon, J.-H., Wang, S.-Y.S., Gillies, R.R., Hipps, Le., Kravitz, B., Rasch, P.J., 2015. Extreme fire season in California: a glimpse into the future? Bull. Am. Meteor. Soc. 96, S5–S9.

Young, A.M., Higuera, P.E., Duffy, P.A., Hu, F.S., 2017. Climatic thresholds shape northern high-latitude fire regimes and imply vulnerability to future climate change. Ecography 40, 606–617.